JOURNAL OF GEOPHYSICAL RESEARCH: ATMOSPHERES, VOL. 118, 4834–4846, doi:10.1002/jgrd.50381, 2013

On the potential high acid deposition in northeastern China

Junji Cao,[1] Xuexi Tie,[1,2] Walter F. Dabberdt,[3] Tang Jie,[4] Zhuzi Zhao,[1] Zhisheng An, Zhenxing Shen,[5] and Yinchang Feng[6]

Received 27 September 2012; revised 26 March 2013; accepted 30 March 2013; published 30 May 2013.

[1] There is an acid deposition conundrum in China: contrary to conventional wisdom, extremely high ambient sulfate concentrations in northeastern China are not always accompanied by correspondingly high acidities. To investigate this discrepancy, data from two independent sets of *in situ* field measurements were analyzed along with Scanning Imaging Absorption Spectrometer for Atmospheric Chartography (SCIAMACHY) satellite observations and Model for Ozone and Related chemical Tracers (MOZART) chemical transport model calculations. The field measurements included soluble aerosol ion concentrations and pH and particulate data from 11 cities, as well as pH measurement data from 74 sites in China. This study explores the basis for and the impacts of the large discrepancy in northeastern China between the major acidity precursors (SO_2 and NOx) and measured acidity levels as indicated by pH values. There are extremely high SO_2 emissions and ambient concentrations in northeastern China, while the corresponding acidity is unusually low (high pH) in this region. This is inconsistent with the usual situation where high-acidity precursor pollutants result in low pH (high acidity) values and acid rain conditions. In other regions, such as southern China and the United States, high SO_2 concentrations are typically well correlated with high acidities. Using measured soluble particle measurements (including both positively and negatively charged ions), it is seen that there are high values of alkaline ions in northeastern China that play an important role in neutralizing acidity in this region. This result strongly suggests that the high alkaline concentrations, especially Ca^{2+}, increase warm season pH values by about 0.5 in northern China, partially explaining the inconsistency between sulfate concentrations and acidity. This has a very important implication for acid rain mitigation—especially in northeastern China. However, there are additional issues pertaining to the precursor-acidity relationship that need further investigation. Why is it that the reduction in acidity due to the alkaline ions is only significant in summer? During winter, the measured alkaline ions play a much smaller role in explaining the discrepancy. The measured alkaline ions in this study were mostly obtained from particles in the $PM_{2.5}$ range. However, the size of calcium particles is typically much larger—extending well beyond 2.5 μm—and so a significant amount of calcium may be underestimated by $PM_{2.5}$ measurements alone. The under-sampling of calcium particles is further exacerbated in that the sampling protocol excluded particle (and soluble ion and pH) measurements during dust storms. This all leads to the need for an improved understanding of pollutant-ion-particulate interactions in China, and their role in explaining the counter-intuitive conclusion that dust mitigation strategies in China could have the unintended consequence of exacerbating acid rain conditions.

Citation: Cao, J., X. Tie, W. F. Dabberdt, T. Jie, Z. Zhao, Z. An, and Z. Shen (2013), On the potential high acid deposition in northeastern China, *J. Geophys. Res. Atmos.*, *118*, 4834–4846, doi:10.1002/jgrd.50381.

[1]Key Laboratory of Aerosol Science and Technology, SKLLQG, Institute of Earth Environment, Chinese Academy of Sciences, Xian, China.
[2]National Center for Atmospheric Research, Boulder, Colorado, USA.
[3]Vaisala Inc., Boulder, Colorado, USA.
[4]Chinese Academy of Meteorological Sciences, Xian, China.
[5]Xi'an Jiaotong University, Xian, China.
[6]State Environmental Protection Key Laboratory, Nankai University, China.

Corresponding author: X. Tie, NCAR, PO BOX 3000, Boulder, CO 80303, USA. (xxtie@ucar.edu)

2169-897X/13/10.1002/jgrd.50381

1. Introduction

[2] There is an acid rain conundrum in northeastern China: extremely high sulfate concentrations are not accompanied by very high acidities. Several studies have previously shown that, despite extremely high sulfur and sulfate concentrations in northeastern China, acidity levels are low in this region [*Wang and Wang*, 1996; *Tang et al.*, 2010]. At the same time, high sulfur and sulfate concentrations in southern China are not accompanied by low acidity. The reasons for this inconsistency between high acidity precursors and low acidity

levels in northeastern China are not well understood. To investigate this contradiction, data were analyzed from two sets of *in situ* field measurements that included soluble aerosols, pH, and particulates in 11 cities and pH measurements at another 74 sites across China together with Scanning Imaging Absorption Spectrometer for Atmospheric Chartography (SCIAMACHY) satellite observations and Model for Ozone and Related chemical Tracers (MOZART) model calculations.

[3] According to the U.S. Environmental Protection Agency, "'acid rain" is a broad term referring to a mixture of wet and dry deposition (deposited material) from the atmosphere containing higher than normal amounts of nitric and sulfuric acids" (http://www.epa.gov/acidrain/what/index.html). Acid rain damages the environment. It causes acidification of lakes and streams and contributes to the damage of trees and sensitive forest soils. In forests, acid rain that seeps into the ground can dissolve important nutrients such as magnesium (Mg) and calcium (Ca). Acid rain increases the acidity of lakes and streams, which is often lethal to aquatic wildlife. And acid rain accelerates the decay of construction materials and paints, damaging buildings, monuments, and vehicles.

[4] Precipitation is acidified by two common air pollutants: sulfur dioxide (SO_2) and nitrogen oxides ($NO_X = NO + NO_2$). Both SO_2 and NOx are emitted to the atmosphere by natural and anthropogenic processes. Natural emissions of SO_2 include volcanic eruptions and biomass burning, while anthropogenic emissions are mainly due to the combustion of coal and oil, which account for more than 75% of global SO_2 emissions [*Chin et al*., 2000]. Within China over the period 1996–2010, coal combustion has been the single largest contributor (89%–93%) to SO_2 emissions [*Lu and Streets*, 2011]. The variability over this 15 year period reflects changes in the use of coal, the growth in China's economy, and the introduction of flue gas desulfurization technology. Natural emissions of NO_x include lightning and biomass burning (both natural and anthropogenic) [*Brasseur et al*., 1998; *Bond et al*., 2002; *Tie et al*., 2002; *Horowitz et al*., 2003]. Anthropogenic emissions of NO_x are mainly from coal and oil combustion, which account for more than 75% of global emissions [*Emmons et al*., 2010]. Within China, coal and oil combustion accounted for 90% of NOx emissions in 2010. For example, in the capital city of Beijing, the number of vehicles increased from 0.9 million in 1994 to 2.7 million in 2005, which led to large increases in NO_x emissions [*Chan and Yao*, 2008]. In Shanghai, the GDP (Gross Domestic Product) increased 15.6 times from 1990 to 2007, accounting for more than 5% of the total GDP in China [*SMSB*, 2008]. As a consequence, NO_x emissions have increased rapidly; in the six-year period from 1990 to 1996, NO_x emissions nearly doubled, increasing from 2.8×10^5 tons to 4.8×10^5 tons [*Chan and Yao*, 2008].

[5] In 2009, coal usage was about 2.01 billion metric tons, accounting for 70% of China's total energy consumption [*IEA*, 2010]. This has led to high SO_2 emissions, resulting in the high ambient concentrations of SO_2 [*Kawamoto et al*., 2004]. One of the major fates of SO_2 gas is to form sulfate particles; understanding their formation in the troposphere is critical because of effects on human health and climate [*Zhao et al*., 2006; *Tie et al*., 2009]. Quantifying the SO_2 budget—emissions, transformations, and deposition—is an important environmental issue in China.

[6] The large increases in China's anthropogenic emissions of SO_2 and NO_x have been a consequence of the country's rapid economic development, especially in the large cities and provinces in eastern China. From a national GDP of US $1.20T in 2000, China's GDP nearly doubled to US$2.26T in 2005 and then more than doubled again in 2010 to $5.93T. The spike in China's growth during the latter half of the past decade is projected to decrease yet the International Monetary Fund projects, it will still average about nine percent per annum through 2015, which will certainly be accompanied by additional challenges to China's acid rain and other atmospheric pollution problems (http://www.forbes.com/sites/billconerly/2011/12/19/chinas-economic-forecast-2012-2013-a-business-perspective/).

2. Measurements and Modeling

2.1. Acidity Measurements

[7] Ambient SO_2 and NO_x gasses can be oxidized into sulfates (H_2SO_4) and nitrates (HNO_3). And when sulfates and nitrates are entrained into rain, snow, and fog droplets, they form acidic ions, such as SO_4^{2-} and NO_3^- by the following processes:

$$H_2SO_4 \rightarrow 2H^+ + SO_4^{2-}, \text{ and } HNO_3 \rightarrow H^+ + NO_3^-$$

thereby rapidly increasing the acidity of the hydrometeors.

[8] The China Meteorological Administration's (CMA) Acid Rain Monitoring Network (ARMN) has routinely measured pH from 1992 to 2005 at 74 sites across China. Of these sites, 37 are located in densely populated areas, including provincial capitals and large cities (populations greater than one million). The remaining 37 are located in sparsely populated areas, and include three World Meteorological Organization-Global Atmosphere Watch regional stations and three mountaintop weather stations. Precipitation acidity and conductivity were routinely measured at those 74 stations. The instrumentation, sampling, calibration, and other operations are all regulated according to the CMA standard operations manual [1992; 2005]. Precipitation samples were collected at the meteorological sites using polyethylene polymer buckets of 40 cm diameter. The upper rims of the buckets are installed at the height of 1.2 m above ground. Following the sampling protocol in place through 2005, samples were collected during precipitation events (>1 mm) only. Inter-comparisons of blind samples are organized annually by the CMA's central laboratory. Data verification and validation were performed according to procedures described by *Tang et al*. [2010]. The measured pH values from 2003 have been used here, which is consistent with the ion species measurements described below.

[9] For comparison purposes, pH measurements were also obtained for 2003 from the 135 station network of the U.S. National Acid Deposition Program (NADP). As with the China data, annual-average pH values were similarly calculated from the measured data. Samples were collected continuously using a wet deposition collector, which opens automatically during wet weather, allowing the precipitation to fall into a collection bucket, and then closes as soon as the precipitation ends. The samples were first weighed at the field laboratories and then transferred to the Central Analytical Laboratory (CAL) in Champaign, Illinois. Each field site

Table 1. Cities (and Approx. Coordinates) Comprising the 11-Station Network Used to Measure pH and Various Soluble Ions (See Also Map in Figure 5)

Site	Lat (°N)	Lon (°E)
Hong Kong	22.25	114.17
Beijing	39.93	116.28
Chongqing	29.52	106.48
Yulin	22.63	119.15
Tianjin	39.14	117.18
Qingdao	36.10	120.37
Wuhan	30.58	114.27
Guangzhou	23.12	113.25
Shanghai	31.01	121.41
Hangzhou	30.26	120.17
Xi'an	34.16	108.95

is also equipped with a weighing-bucket rain gage that provides a continuous record of rainfall amounts (resolved to 0.25 mm). The rain gage also monitors the wet deposition collector, recording whether the collector was properly open during wet periods and closed during dry periods. All the samples were sent to the CAL for analysis and data entry, verification, and screening. The CAL measures free acidity (pH) and ions in the rainwater. Finally, the CAL delivers all data and information to the NADP Program Office, which applies a final set of checks and resolves remaining discrepancies. Data are then made available on the NADP Web site (http://nadp.sws.uiuc.edu).

2.2. Soluble Ion Measurements

[10] In order to gain greater insight into the cause of the pH-precursor inconsistency in northeastern China, a special *in situ* network was established to measure various soluble ions (including sulfates, nitrates, and the important positive ions of Ca^{2+}, Na^{+}, K^{+}, and Mg^{2+}). Measurements were made in 11 cities (Table 1) across China during January and July 2003. During the measurement periods, daily 24 h $PM_{2.5}$ samples were collected by battery-powered mini-volume samplers (Airmetrics, Euegene, Oregon, USA). The instruments were operated at a flow rate of 5 l min^{-1} [*Cao et al.*, 2005]. Samples were collected on 47 mm quartz microfiber filters (Whatman QM/A, Maidstone, UK), which were precombusted at 900°C for 3 h to remove contaminants prior to sampling. After collection, the loaded filters were transferred to the laboratory of the Institute of Earth and Environment (IEE), China, and placed in clean polystyrene Petri dishes and stored at 4°C to prevent evaporation of volatile components. Each filter sample was used for gravimetric determination of aerosol mass concentration; each filter aliquot was equilibrated for 24 h at room temperature (20–23°C) and relative humidity of 35–45%. The IonPac CS12A column and IonPac AS14A column instruments were used to determine ion concentrations. Standard reference materials produced by the National Research Center for Certified Reference Materials (Beijing, China), were analyzed for quality control. All reported ion concentrations were calibrated against field blanks. Because these soluble ion concentrations were not measured by the CMA's pH network, they provide useful information for better understanding the processes controlling acidity levels. It should be noticed that there is an assumption that these measured ions can be dissolved in rain water. In other words, the measured result provided "background" acidity information, instead of in-situ ions in precipitation water.

2.3. MOZART Model

[11] MOZART (Model for Ozone and Related chemical Tracers; [*Horowitz et al.*, 2003; *Emmons et al.*, 2010]) is a global chemical transport model that was used to calculate the distribution of SO_2 and NO_x as well as their chemical transformation to sulfates and nitrates. Values of pH were also calculated with the MOZART model (following *Tie et al.* [2005]), and subsequently compared with the *in situ* measurements. In the pH calculation, the model accounts for both the important gas to aqueous phase conversions and the oxidation processes in aqueous phase. For example, the dissociation of HNO_3 is included in the calculation, which enhances the gas to aqueous conversion by a factor of 10^5. Two geographical regions—the U.S. and China—were compared in order to investigate conditions in different settings given that the U.S. had successfully initiated a National Acid Precipitation Assessment Program nearly three decades ago while China has just recently begun an acid rain mitigation program.

[12] The chemical mechanism in MOZART includes oxidation schemes for non-methane hydrocarbons: ethane, propane, ethene, propene, isoprene, α-pinene, and n-butane. The 85 chemical species simulated by MOZART are listed in Table 2 of *Emmons et al.* [2010]. Heterogeneous reactions of N_2O_5 and NO_3 on sulfate aerosols are included, and aerosol concentrations are also calculated in the model [*Tie et al.*, 2001]. The uncertainty in the reaction coefficient of N_2O_5 ranges from 0.01 to 0.1; however, while the heterogeneous conversion from N_2O_5 to HNO_3 is important at high-latitudes, it is of minor importance in low-to-mid latitudes [*Tie et al.*, 2003] such as northeastern China. Surface emissions of chemical species used in MOZART include those from fossil fuel burning and other industrial activity, biomass burning, biogenic emissions from vegetation and soils, and oceanic emissions. The 2003 global surface emissions used in the model are summarized in Tables 9 and 10 of *Emmons et al.* [2010] and include 99.3 Tg NO and 151.8 Tg SO_2.

[13] By including SO_2 and NO_x chemistry and the chemical transformation from gasses to aerosol particles in MOZART [*Tie et al.*, 2005; *Emmons et al.*, 2010], the pH values could be calculated using the scheme of *Seinfeld and Pandis* [2006], where

$$[H^+] + [NH_4^+] = [OH^-] + [HCO_3^-] + [NO_3^-] + [HSO_3^-] + [2SO_3^{2-}] + [2SO_4^{2-}] \quad (1)$$

and

$$pH = -\log([H^+])$$

[14] In equation 1, the positive (alkaline) ion NH_4^+ accounts for the effect of ammonia to decrease acidity. The hydroxide ion OH^- occurs due to the ionization of water (H_2O). The hydrogen carbonate ion HCO_3^- is produced by dissolved CO_2 in water. The nitrate ion NO_3^- is

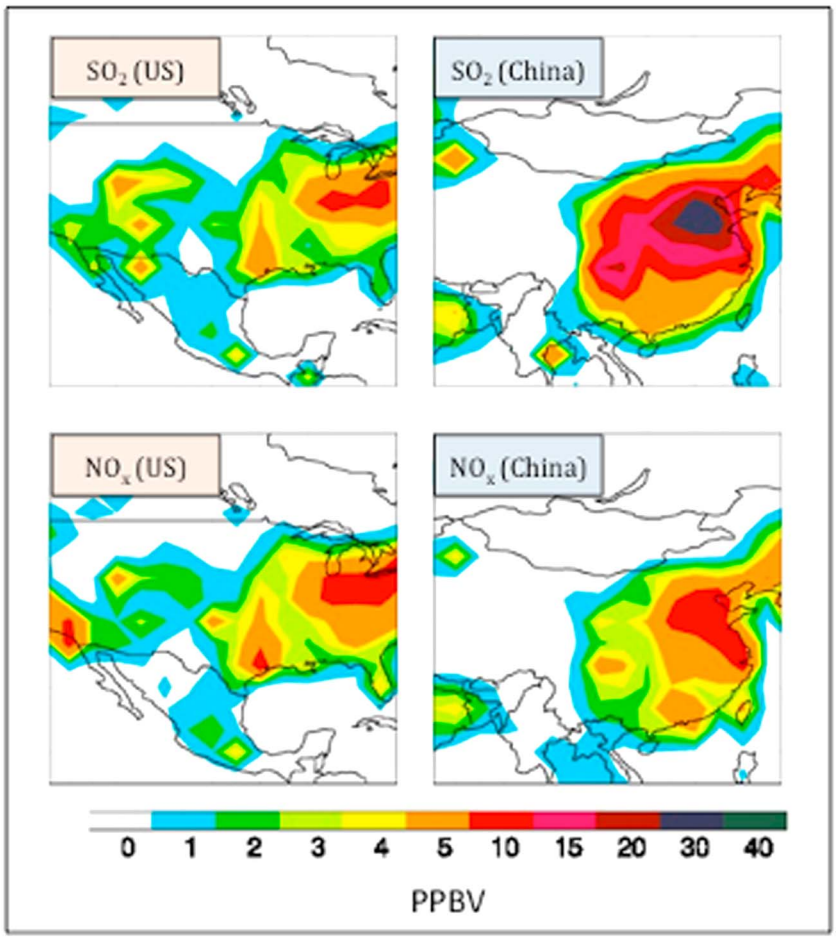

Figure 1. MOZART-calculated surface concentrations (ppbv) of SO_2 and NO_x in eastern China (right-hand panels) and the eastern U.S. (left-hand panels).

produced by dissociation of nitric acid (HNO_3) in water. HSO_3^- and SO_3^{2-} are the products formed by dissolved SO_2 gas in water. And SO_4^{2-} results from the dissociation of sulfate particles in water. There are two very relevant implications of this equation. First, the SO_2 effect is very important due to both the dissolved gas SO_2 in water and the dissociation of sulfate particles. There is also a factor of two associated with SO_3^{2-} and SO_4^{2-} in equation 1, as each of these species contains two negative ions. Second, in the ambient atmosphere, there are several positive ions, such as Ca^{2+}, Na^+, K^+, and Mg^{2+}, which are not included in the model. As a result, the model calculation of the pH values assumes that these positive ion concentrations are relatively small and have only a minor effect on pH, which may not always be the case.

[15] MOZART was used to understand the impact of the major air pollutants SO_2 and NO_x on acid precipitation in China. To gain greater understanding, we also used MOZART to simulate conditions in the U.S. to compare differences between the two countries in terms of pollutant precursors and the resulting acidity. As described by *Emmons et al*. [2010], the SO_2 emissions in China and used in MOZART are significantly greater than those in the U.S. For example, the annual emission of SO_2 in the U.S. is about 18 Tg, which is about 10% of the annual global emissions. In contrast, the annual emissions of SO_2 in China are about 40 Tg, about 25% of annual global emissions.

[16] Unlike SO_2, NO_x emissions (expressed as NO) show smaller differences between the U.S. and China. The annual emission of NO_x in the U.S. is about 12 Tg NO, accounting for about 13% of global NO_x emissions, which is similar to emissions in China (15 Tg NO, or 17% of the global annual average). Also, the geographic distribution is somewhat similar in the two countries with higher emission densities of both SO_2 and NO_x located in eastern parts of China and the U.S.

3. Results and Discussion

3.1. MOZART Simulations and Comparisons With Observations

[17] With high SO_2 and NO_x emissions in both eastern China and the U.S., there are corresponding, relatively high annual-average SO_2 and NO_x surface concentrations in these regions. Figure 1 illustrates the calculated SO_2 concentrations, which are highest in eastern China with a maximum value of ~30 ppbv. In contrast, the SO_2 concentrations in the eastern U.S. are significantly smaller than those in eastern China, with a maximum value of only ~10 ppbv. The calculated NO_x concentrations, however, show some similarity between eastern China and the U.S., with a maximum value of ~10 ppbv in both regions. This result is consistent with the earlier findings of *Tie et al*. [2006].

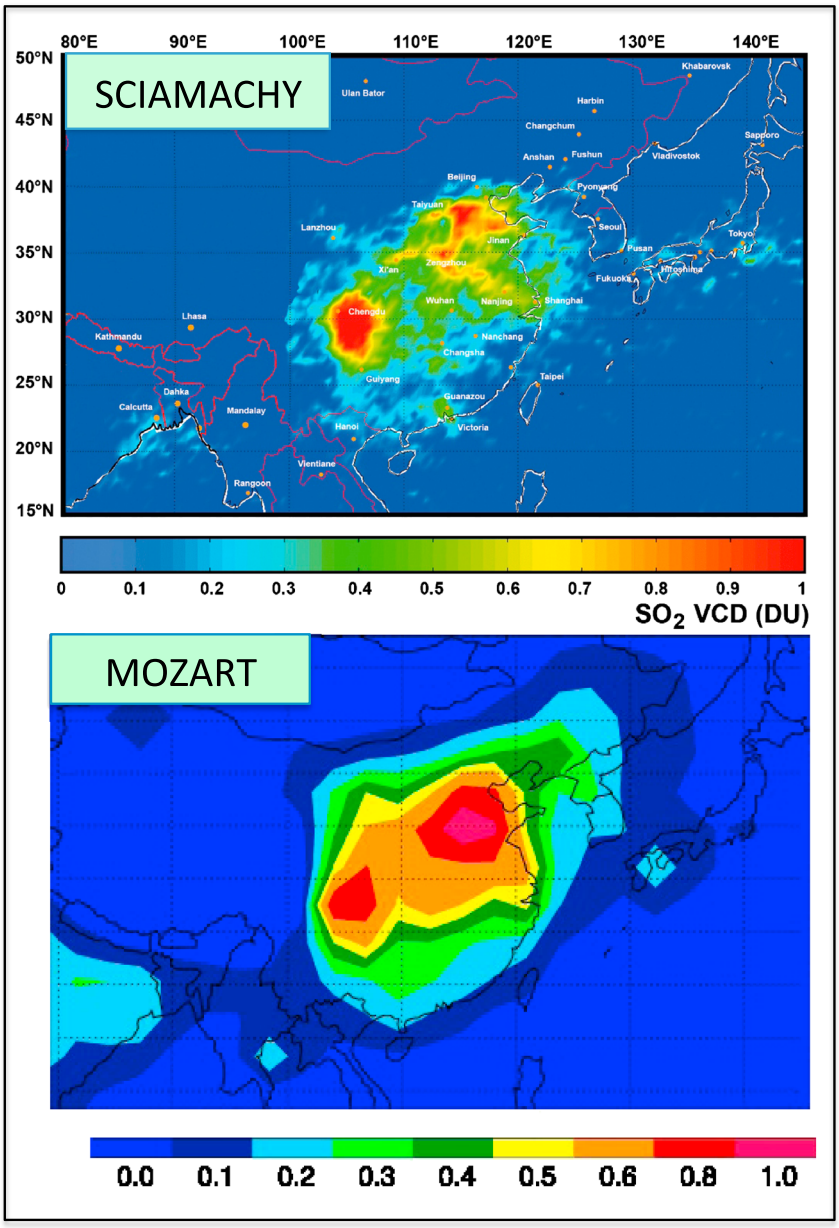

Figure 2. The 2003 annual-average SO_2 column distribution measured by SCIAMACHY and corresponding MOZART-calculated values in eastern China.

[18] The MOZART calculations were also compared to satellite measurements to evaluate the representivity of the model results. Column-integrated values of SO_2 were obtained from the SCIAMACHY imaging spectrometer aboard the European Space Agency's Envisat satellite that was launched in 2002. Envisat flies in a sun-synchronous polar orbit at an altitude of about 800 km, and the repeat cycle of the orbit provides complete global coverage about every three days. The detailed retrieval process and uncertainty of the SCIAMACHY columnar data is documented by *Bovensman et al*. [1999]. The MOZART-SCIAMACHY comparison for eastern China (Figure 2) indicates fair similarity for the horizontal distribution of column SO_2. For example, there are two local maxima of SO_2 concentration in both the modeled and measured results. The first high is centered in northeastern China, and the second is located in mid-south China (Sichuan Province). However, there are also some discrepancies between the simulations and measurements. For example, the maximum in central China is overestimated, while the maximum in southern China is slightly underestimated. The modeled distribution displays a more diffuse pattern than the measured distribution, largely due to the coarse resolution of the model (2.8° by 2.8° in latitude and longitude). Also, the area of high concentrations in northeastern China has a larger spatial extent than indicated by the SCIAMACHY retrievals.

[19] To demonstrate the representativeness of the calculated pH values, the calculated pH values using equation 1 are compared with the corresponding measured values in the U.S. at the 135 NADP sites (see the upper panel of Figure 3). Both the modeled and measured results represent annual-average values. It can be seen that the measured and

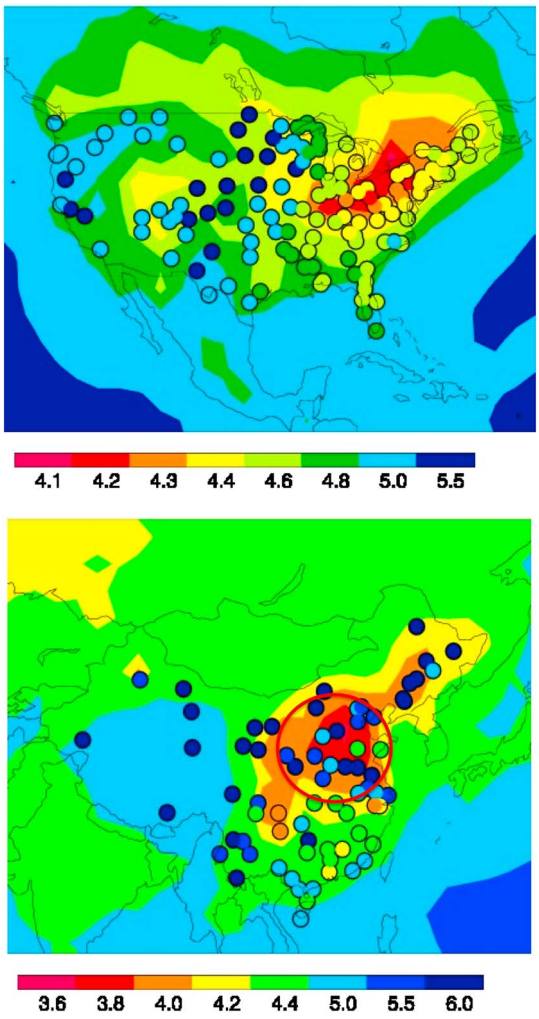

Figure 3. Measured (circles) and MOZART-calculated pH values using equation 1 (contour lines) in the U.S. (upper panel) and China (lower panel). The large red circle indicates the area where there is a significant discrepancy between measured and calculated pH values.

calculated pH patterns are spatially consistent with acidity highest in northeastern U.S. Both measured and calculated minimum pH values are in the range 4.2–4.6. The high acidity values are closely related to high concentrations of SO_2 and NO_x in this region (Figure 1) where both the SO_2 and NO_x concentrations range from 5 to 10 ppbv. However, some discrepancies are also noticeable. For example, the calculated maximum is overestimated compared to the measured pH values. The second high-acidity region is located in southeastern U.S., with pH values ranging from 4.4 to 4.8. In this region, the SO_2 concentrations vary from 3 to 4 ppbv, and the NO_x concentrations vary from 3 to 5 ppbv, which are less than half the respective concentrations in the northeast. In northwestern U.S., the acidity is weakest, with pH values ranging from 4.8 to 5.5. As shown in Figure 1, the concentrations of SO_2 and NO_x in this region are lowest (less than ~1 ppbv), yielding low acidities in this region. In the middle of the U.S., the calculated pH values are generally higher than the measured results.

[20] The lower panel of Figure 3 indicates that the measured pH values are reasonably well simulated with MOZART. Despite overall agreement between the model results and the most important features of the measurements, there are also some discrepancies. For example, the model results show less of the fine scale features due to the coarse horizontal resolution of the model. The general consistency between the calculations and measurements suggests that the pH values can be reasonably well simulated by MOZART together with the Seinfeld-Pandis relationship (equation 1). As a result, we are confident in concluding, in general, that SO_2 and NO_x play the major role in determining acidity in the U.S., while the positive ions Ca^{2+}, Na^{+}, K^{+}, and Mg^{2+} play only a minor role in the U. S. because of their low concentrations. However, there is an exception in the middle of the U.S. where the modeled pH values range from 4.4 to 4.6, while the measured values are about 5.5. This overestimation of acidity in the middle U. S. suggests that positive ions might play an important role in reducing the acidity in this region as the wet deposition measurements indicate that the concentrations of Ca^{2+} in rain water are significantly higher than in the eastern U.S.

[21] As will be seen, the situation is quite different in China. Figure 4 compares the distribution of the measured and calculated pH values in China and its neighboring countries. Unlike the model results in the U.S., the calculated pH values in China are not consistent with the measured values. For example, the *calculated* acidity is highest in northeastern China, with pH values ranging from 3.8 to 4.0. These calculated acidities are consistent with the high SO_2 and NO_x concentrations calculated for this region. As seen in Figure 1, the maximum modeled SO_2 and NO_x concentrations are 30 and 10 ppbv, respectively, resulting in high calculated acidities in this region. However, the

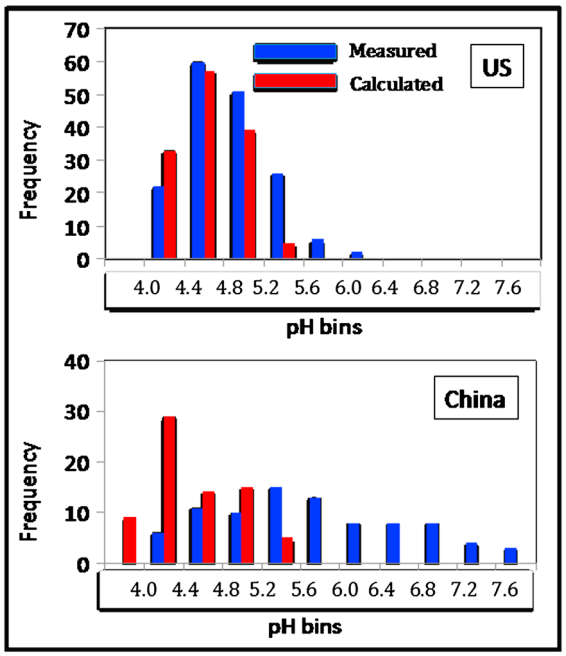

Figure 4. Measured (blue bars) and calculated (red bars) pH occurrence frequency (%) in the U.S. (upper panel) and China (lower panel). Data are from the 135 NADP sample sites in the U.S. and the 74 CMA-ARMN sites in China.

Table 2. The Measured Mean Concentrations ($\mu g/m^3$) of Various Soluble Ions in 11 Cities Across China During January and July, 2003

City	$PM_{2.5}$	Na^+	NH_4^+	K^+	Cl^-	NO_3^-	SO_4^{2-}	Ca^{2+}	Mg^{2+}	pH
					January–July Averages					
HK	65.06	0.58	5.44	0.90	1.01	6.14	14.99	3.71	0.26	5.47
BJ	148.76	1.48	12.26	1.82	3.50	14.90	24.81	2.32	0.27	5.09
CQ	253.31	1.59	21.99	4.76	7.66	12.44	51.37	1.22	0.29	4.32
YL	140.73	3.83	6.24	2.14	0.87	6.38	15.28	1.80	0.30	6.23
TJ	160.43	3.77	16.48	2.22	9.74	18.83	31.83	5.32	0.36	5.62
QD	107.14	1.46	11.11	1.83	3.12	14.80	20.34	1.74	0.13	5.00
WH	144.41	1.99	12.61	3.04	2.97	17.46	24.16	1.33	0.07	4.80
GZ	133.18	1.95	8.46	2.43	2.93	10.03	20.78	2.66	0.23	4.77
SH	124.34	1.73	10.16	2.30	4.35	12.77	20.56	1.65	0.24	5.96
HZ	133.78	1.62	11.19	3.90	2.60	14.93	24.99	2.03	0.25	4.35
XA	236.10	2.29	18.87	3.30	4.95	17.83	39.30	4.54	0.45	6.75
					Winter (January)					
HK	102.71	0.54	10.69	1.14	0.62	11.26	26.00	2.21	0.24	5.21
BJ	161.60	2.00	16.00	1.40	5.70	19.90	29.50	1.70	0.30	4.47
CQ	356.57	2.24	33.36	6.55	13.12	19.32	70.78	1.22	0.31	4.10
YL	231.30	3.10	11.60	3.70	0.90	10.70	20.50	1.30	0.30	5.82
TJ	206.70	3.20	23.20	3.10	13.60	27.00	38.90	2.30	0.40	5.24
QD	186.30	2.68	20.61	3.28	5.54	27.67	34.29	1.17	0.14	4.60
WH	227.10	3.40	22.70	3.80	5.30	32.50	36.60	1.30	0.10	4.60
GZ	222.20	3.50	15.80	3.80	5.30	18.90	35.40	3.30	0.20	4.33
SH	195.70	2.60	16.60	3.00	7.70	24.00	27.50	2.00	0.30	5.90
HZ	182.50	2.60	17.10	5.00	4.40	24.10	33.00	2.20	0.30	4.00
XA	348.20	2.20	30.70	4.60	8.80	28.80	55.20	3.70	0.50	6.70
					Summer (July)					
HK	27.42	0.61	0.20	0.65	1.40	1.02	3.97	5.22	0.27	5.72
BJ	135.9	0.90	8.50	2.20	1.30	9.90	20.10	2.90	0.30	5.70
CQ	150.1	1.00	10.60	3.00	2.20	5.60	32.00	1.20	0.30	4.53
YL	50.14	4.55	0.88	0.55	0.87	2.08	10.02	2.34	0.30	6.64
TJ	114.21	4.38	9.73	1.36	5.92	10.62	24.75	8.34	0.34	6.00
QD	27.99	0.24	1.61	0.39	0.70	1.93	6.40	2.31	0.11	5.40
WH	61.70	0.50	2.50	2.30	0.60	2.40	11.70	1.40	0.00	5.00
GZ	44.20	0.40	1.10	1.10	0.50	1.20	6.20	2.00	0.20	5.21
SH	53.00	0.90	3.70	1.60	1.00	1.50	13.60	1.30	0.20	6.03
HZ	85.00	0.60	5.30	2.80	0.80	5.80	16.90	1.80	0.20	4.70
XA	124.10	2.37	7.02	1.97	1.07	6.91	23.37	5.40	0.41	6.8

HK, Hong Kong; BJ, Beijing; CQ, Chongqing; YL, Yulin; TJ, Tianjin; QD, Qingdao; WH, Wuhan; GZ, Guangzhou; SH, Shanghai; HZ, Hangzhou; XA, Xi'an.

corresponding *measured* pH values show considerably lower acidities, with pH ranging from 5 to 6 in this region. In southeastern China, on the other hand, the calculated and measured acidity values show much better agreement (except along the south coast of China). For example, the calculated pH values range from 4.2 to 4.4, and the measured values range from 4.2 to 5.0. In the remote western regions of China, both calculated and measured acidities are low (pH ~5.0) due to the correspondingly low SO_2 and NO_x concentrations.

[22] The differences between observations and model-calculated pH are greatest in northeastern China (indicated by the red circle in Figure 3). This discrepancy implies that equation (1) cannot be used to properly calculate the pH values in this region. The acidity should be highest in northeast China owing to its high concentrations of SO_2 and NO_x. However, measurements in this region show considerable low acidity, which in inconsistent with the physical processes inherent in equation 1. Yet in the eastern U.S., it was clearly seen that acidity is proportional to the concentrations of SO_2 and NO_x. A likely reason for this discrepancy is that the concentrations of the positive ions (Ca^{2+} and NH_4^+) are considerably higher in eastern China than in eastern U.S. For example, the averaged positive-negative ion ratio, $(Ca^{2+} + NH_4^+)/(SO_4^= + NO_3^-)$, is 0.12 for the eastern U.S. but 0.37 for eastern China. Accordingly, these positive ions can be neglected in the acidity calculations in the U.S., while they cannot be ignored in China (especially in northeastern China).

[23] The nature of pH distributions in China and the U.S. is further explored using the frequency distributions of the measured and calculated annual mean pH values at the 74 CMA sites and the 135 NADP sites. The comparison (Figure 4) shows that calculated frequency of occurrence (%) pH values in the U.S. is in good agreement with the measured high frequency of occurrence for the 4.4–4.8 (primary) and 4.8–5.2 (secondary) pH bins. The measured mean and median pH values are 4.86 and 4.80 in the U.S. sites, compared with calculated values of 4.66 and 4.67. The total range is relatively narrow, with pH values distributed from 4.0 to 6.0. The measured standard deviation (SD) is 0.40 and the calculated SD is 0.31, while the measured and calculated skewness are 1.12 and 1.22, respectively. Unlike the good agreement at the U.S. sites, there are major discrepancies between the measured and calculated frequency distributions in China. The calculated maximum frequency is located in the 4.0–4.4 bin, while the measured maximum lies in the 5.2–5.6 pH bin. The measured mean and median pH values are 5.81 and 5.80, respectively, compared with the calculated values of 4.48 and 4.35—more than an order of magnitude difference in actual acidity. The range of the measured frequency bins (4.2–7.6 pH) is

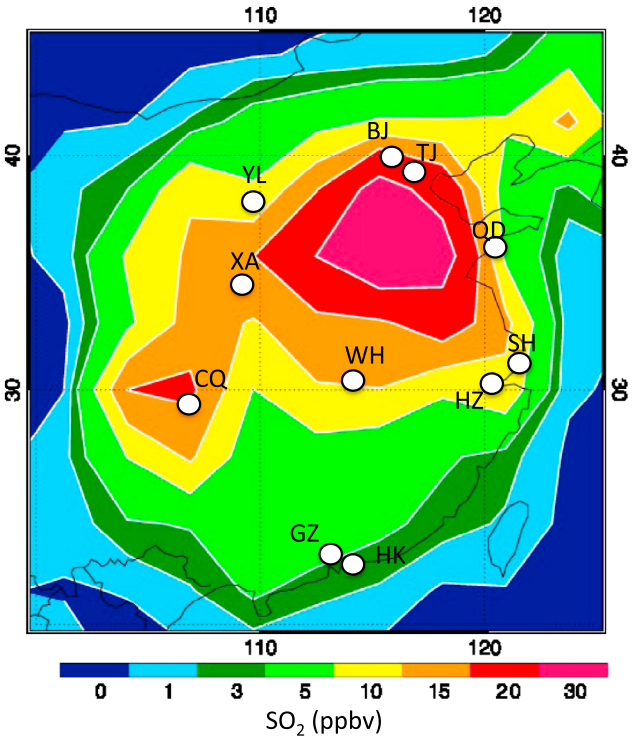

Figure 5. Location of the measurement sites for $PM_{2.5}$, pH and soluble ions in 11 cities across China. The contour lines are the annual-average surface SO_2 concentrations from the MOZART model simulations.

significantly wider than the calculated range (3.8–5.4 pH). The measured SD is 1.03, while the calculated SD is 0.44. And the measured skewness is −0.06, while the calculated skewness is 1.27. These differences in the frequency distributions further point to the important roles of positive ions in neutralizing acidity in northeastern China, which will next be explored through analysis of the detailed ion measurements from the 11 station network.

3.2. The Role of Positive Ions

[24] In order to quantitatively study the important issue of low-acidity and high acidity-precursors (SO_2 and NO_x) in northeastern China, the 11 city *in situ* network was operated during January (winter) and July (summer) of 2003 to measure a suite of soluble ions and pollutants (including pH, sulfates, nitrates, and the positive ions of Ca^{2+}, Na^+, K^+, and Mg^{2+}). The monthly average values are listed in Table 2.

[25] The measured concentrations of $PM_{2.5}$ are very high with monthly average values well in excess of China's new particulate standards (Appendix A). By way of comparison, the U.S. National Ambient Air Quality Standards for $PM_{2.5}$ are 15 $\mu g\,m^{-3}$ (annual average) and 35 $\mu g\,m^{-3}$ (24 h average), and the newly announced (These new PM standards for China were enacted in February 2012 and will take effect for four cities in 2012 and extended to another 113 cities in 2013). Chinese National Ambient Air Quality Standards for $PM_{2.5}$ are 35 $\mu g\,m^{-3}$ (annual average) and 75 $\mu g\,m^{-3}$ (24 h average). The monthly averaged $PM_{2.5}$ concentrations at the 11 sites in China were generally higher than 100 $\mu g\,m^{-3}$, except the HK site (65 $\mu g\,m^{-3}$). For the negative (acidic) ions, the concentrations of SO_4^{2-} were the highest (ranging from 15 to 50 $\mu g\,m^{-3}$), followed by the NO_3^- concentrations (ranging from 6 to 18 $\mu g\,m^{-3}$). Because of the high SO_4^{2-} concentrations and the two ions in each molecule, the sulfate particles are the dominant acidifying species in acid rain in China. In addition to the negative ions, there were also large concentrations of positive (alkaline) ions, which neutralize and so reduce the acidity of acid rain. The seasonal variation of temperature and emissions also plays important roles for NH_4^+ and NO_3^-. As discussed by *Budhavant et al.* [2012] and *Safai et al.* [2010], ammonium nitrate (NH_4NO_3) is more stable in winter than summer because of the lower temperatures. The emissions of the precursors of NO_3^- and SO_4^{2-} are higher in winter than summer due to the higher usage of coal (e.g., heating). The highest concentrations of the positive ions were those of NH_4^+ (ranging from 5 to 22 $\mu g\,m^{-3}$), followed by the concentrations of Ca^{2+} (ranging from 1 to 5 $\mu g\,m^{-3}$), Na^+, and K^+. The higher NH_4^+ levels are attributed to high biochemistry activities, such as urban landfills [*Makar, et al.*, 2009]. The high concentrations of Ca^{2+} are typical in large Chinese cities, partially due to rapid economic development, which leads to a large number of construction sites. These building sites and unpaved or dirt roads often produce large amounts of dust with associated Ca^{2+} emissions.

[26] In addition to construction sites, high concentrations of Ca^{2+} also result from dust storms [*Shen et al.*, 2011]. In the desert region of northwest China and Mongolia, massive dust storms [*Bian et al.*, 2011] often occur that are transported eastward causing high particle concentrations and extremely low visibility. These dust storms have a very strong seasonal variability, often occurring in springtime [*Singer*, 1988; *Gomes and Gillete*, 1993; *Bian et al.*, 2011]. They contain very large particles (up to 50 μm in diameter) and consist of Al, Si, K, Ca, Ti, Mn, Fe, and so forth. [*Xuan and Sokolik*, 2002]. As discussed by *Shao and Dong* [2006], the frequency of dust storms in eastern China ranges from 1 to 10 per annum, depending on location. For example, during 2003, over the source area of Mongolia, there were six dusty days in March, 18 days in April, and 10 dusty days in May [*Chung et al.*, 2005]. As shown by the trajectory study [*Wang et al.*, 2004], the pathway of these Mongolia dust storms were located in northern China, such as YL, XA, BJ, and TJ, but were hardly reached to the measurement sites in southern China. During the periods of the dust storms, the alkaline (such as CA^{2+}) significantly increased [*Kanai et al.*, 2005]. The measurement sites in northern China, such as YL, XA, BJ, TJ, and QD, can be expected to have greater Ca^{2+} concentrations as a result of dust storms than the measurement sites located in southern China (see Figure 5).

[27] The four selected measurement sites depicted in Figure 6 each represent different situations with regard to ion concentrations. At Xi'An (XA), the two-month average concentrations of SO_4^{2-} were the second highest (39 $\mu g\,m^{-3}$) among the 11 cities, but the acidity is low (pH = 6.75). At Tianjin (TJ), the situation is similar to Xi'An, with SO_4^{2-} concentrations being the third highest (32 $\mu g\,m^{-3}$) and also with accompanying low acidity (pH = 5.62). But conditions at Chongqing (CQ) and Hangzhou (HZ)—high concentrations of SO_4^{2-} positively correlated

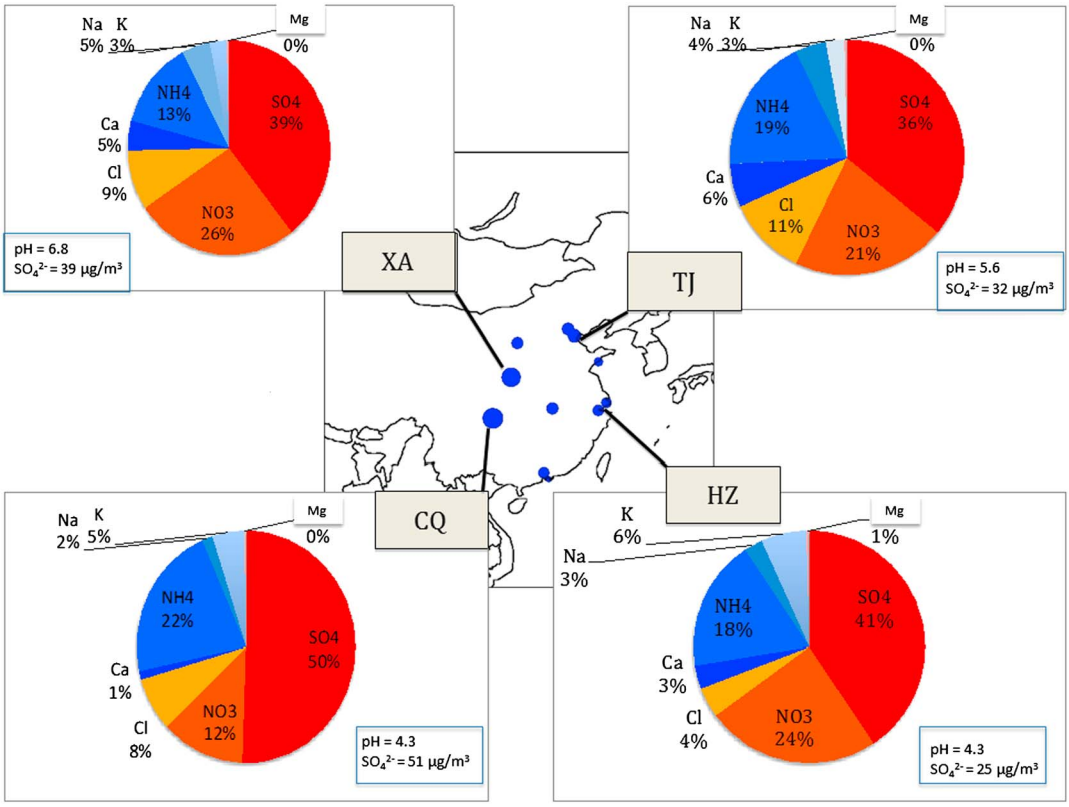

Figure 6. Four selected measurement sites, indicating their respective distributions (January–July average values) of acidic ions (red to yellow colors) and alkaline (blue to gray colors) ions together with pH and sulfate levels. The blue line in the map separates the northern and southern regions.

with high acidity—are very different when compared to Xi'An and Tianjin. At Hangzhou, the SO_4^{2-} concentration was 25 µg m^{-3} with pH = 4.35, while at Chongqing, the SO_4^{2-} concentration was highest (51 µg m^{-3}) among the 11 cities, and the acidity was also highest (pH = 4.32). In the following analysis, we denote the first situation (as observed at XA and TJ) as the "inconsistent" case, and the second (HZ and CQ) as the "consistent" case. The so-called "consistent" case indicates that the concentrations of SO_4^{2-} and acidity are positively correlated, while the "inconsistent" case indicates that they are negatively correlated. The measurement data in Table 2 demonstrate that the "inconsistent" case generally occurs at the more northern sites, while the "consistent" case occurs at the more southern sites.

[28] One of the factors leading to the unusually low acidity observed in northeastern China is the presence of a large amount of alkaline ions, which neutralize the acidity as previously discussed by *Wang and Wang* [1996] among others. As shown in Figure 6 and Table 2, alkaline concentrations are especially abundant in northern China. For example, the concentrations of Ca^{2+} were considerably higher at the northern measurement sites in XA and TJ (4.5 and 5.3 µg m^{-3}, respectively) than at the southern sites in CQ and HZ (1.2 and 2.0 µg m^{-3}, respectively). And since Ca^{2+} contains two positive ions, its neutralizing effect is doubled compared to a single charged ion on an equal molar basis. Although the alkaline concentrations are taken into account in the calculation of the pH values, the alkaline concentrations are still smaller than the acidic concentrations (Figure 6). As a result, the measurements indicate there apparently insufficient positive ions to significantly reduce the acidity in the measured pH values at the sites in northern China. The likely source of this seeming contradiction is the size-cutoff (2.5 µm) of the measured particles. According to the study of *Shen et al.* [2007], the concentrations of Ca^{2+} were found to be significantly higher in total suspended particulates (TSP) than in $PM_{2.5}$ (i.e., particulates less than 2.5 µm in diameter), indicating that Ca^{2+} ion concentrations are higher in the larger sizes (diameter >2.5 µm). Because the ion measurements in the 11 Chinese cities were based on the $PM_{2.5}$ samples, the concentrations of Ca^{2+} likely are significantly underestimated by the measured data. Unlike the other 10 sites, ion concentrations were measured both for $PM_{2.5}$ and PM_{10} particles at the Xi'an site (see Figure 7). Comparing the concentrations of Ca^{2+} in $PM_{2.5}$ and PM_{10} measured at the Xi'an site, it is clear that in the larger PM_{10} particles, the acidic ion concentrations (SO_4^{2-}, NO_3^-, and Cl^-) are smaller than in the $PM_{2.5}$ particles as the ion ratios ($I_{PM10}/I_{PM2.5}$) are less than 2. In contrast, the alkaline ions, especially Ca^{2+}, Na^+, and Mg^{2+}, in the PM_{10} particles are significantly higher than their concentrations in the $PM_{2.5}$ particles. For example, the Ca^{2+} concentration is 5.5 times higher in PM_{10} than in $PM_{2.5}$. As a result, the percentage of Ca^{2+} in the total measured ions increased from 5% in $PM_{2.5}$ to 27.5% in PM_{10}. The ratio ($I_{PM10}/I_{PM2.5}$) of these ion concentrations can be considered an enhancement or scaling factor for estimating the ion concentrations in PM_{10} particles. Due to the lack of PM_{10} measurements in the other ten cities, we applied these ratios (Figure 7) to all of the measurements. In this way, the enhanced Cl^-, K^+,

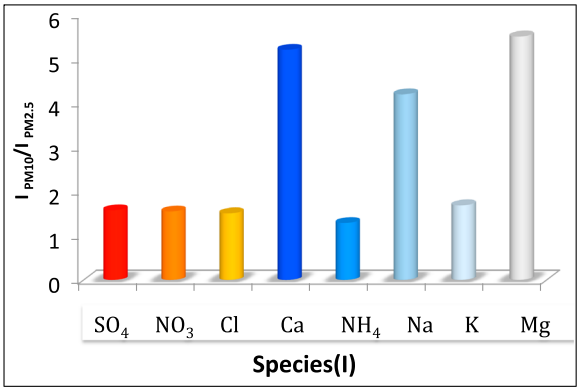

Figure 7. Measured ratio of PM_{10} and $PM_{2.5}$ for different ions at XA, averaged for the months of January and July 2003.

Ca^{2+}, Na^{+}, and Mg^{2+} data were used in equation 1 to study the impact of the scaled ion concentrations, particularly the effect of the alkaline ions on acidity in northeastern China.

[29] Comparison of the measured pH values with the calculated results is illustrated in Figure 8. The calculations include two cases: Case 1 that uses equation 1 but without some of the important alkaline ions (e.g., Ca^{2+}, Na^{+}, etc.); and Case 2 that uses equation 1 with these important alkaline ions. The results indicate that by including these alkaline ions (especially Ca^{2+}), the calculated pH values are improved when compared with the measured pH values. For example, in Case 1, the pH values are underestimated by 0.2–1.4, with an average underestimation of about 1.0. In contrast, the calculated pH values in Case 2 are significantly increased, with the average underestimation reduced to 0.4. This improvement in the calculation of the pH values suggests that these alkaline ions,

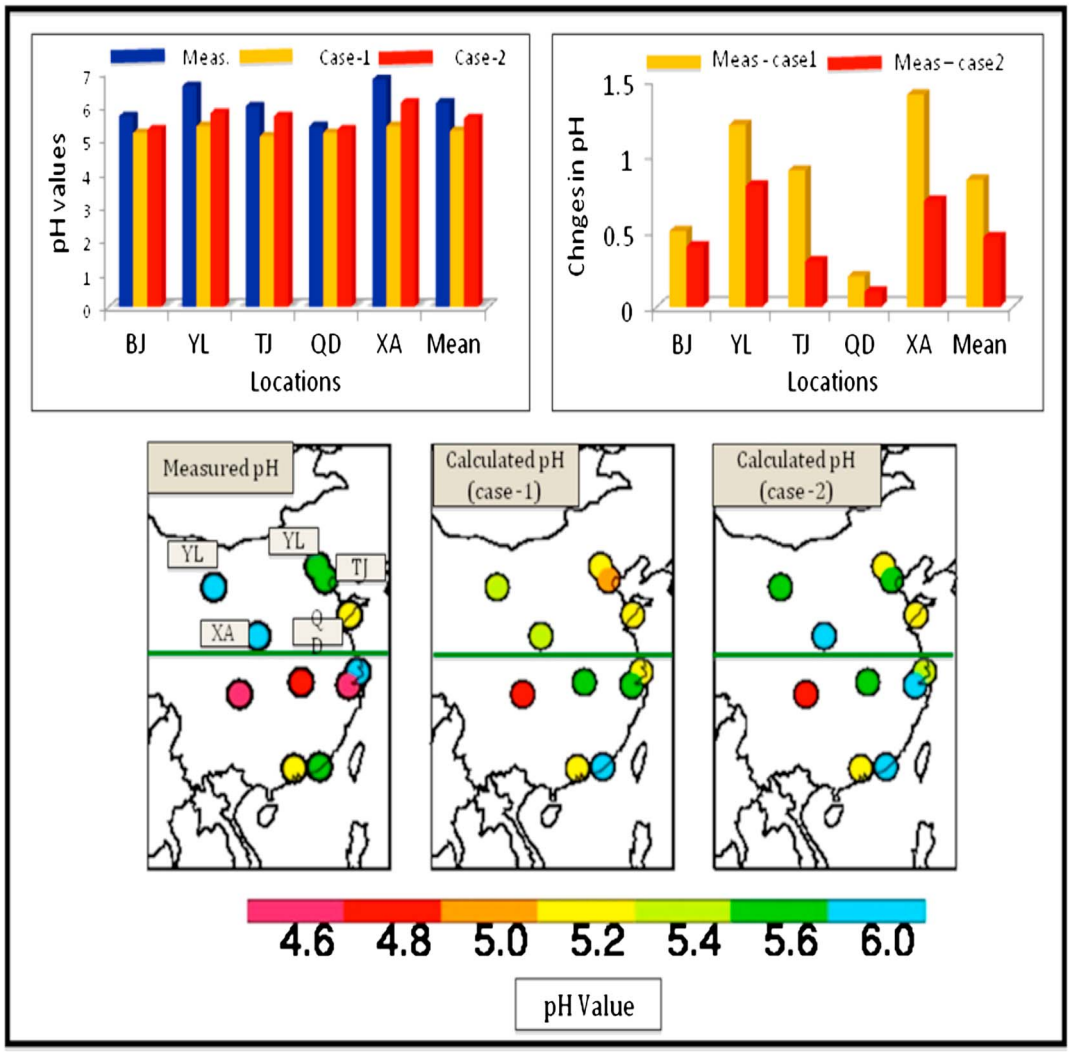

(a) Summer (July)

Figure 8. Measured and calculated pH values using equation 1 without (Case 1) and with (Case 2) the alkaline ions during: (a) summer (July 2003), and (b) winter (January 2003). The lower panels show the geographical distribution at the eleven sites while the two upper panels compare the measured and calculated pH values and their differences at five sites.

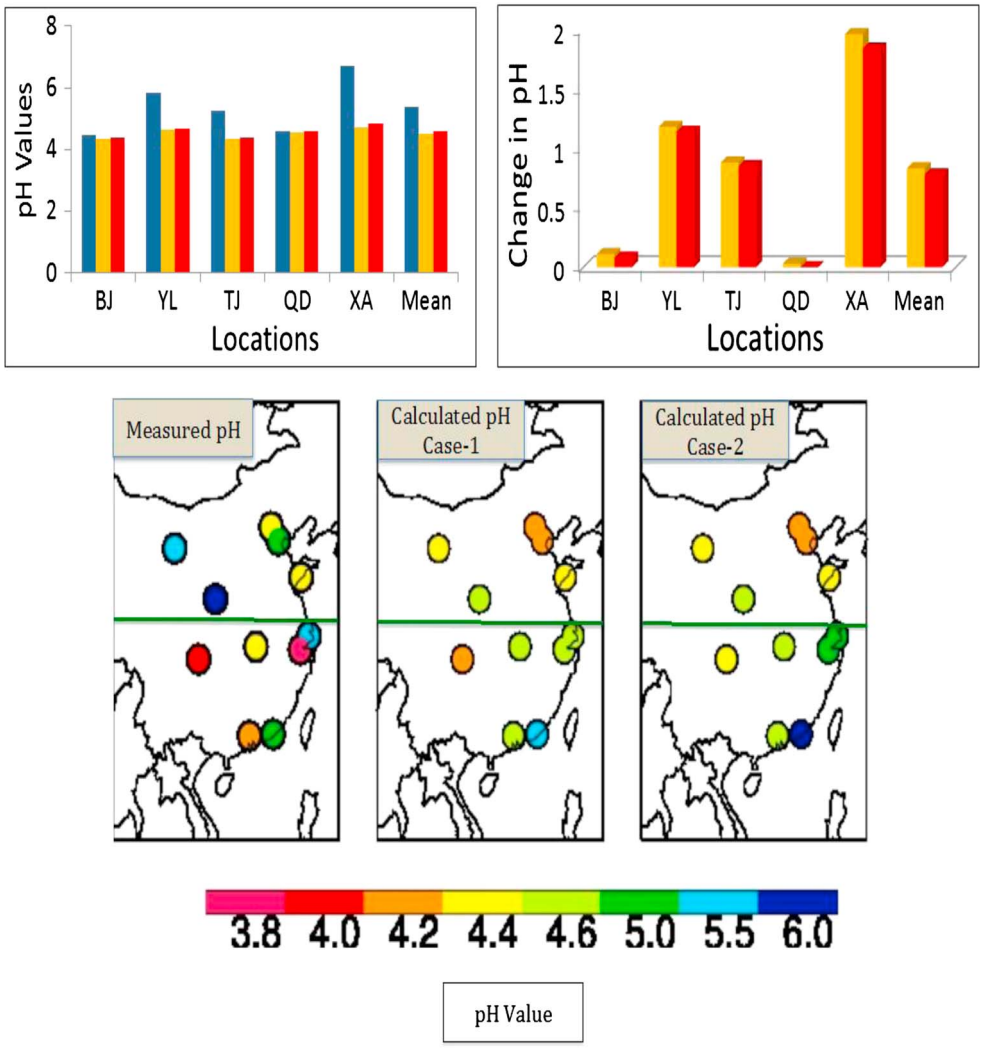

(b) Winter (January)

Figure 8. (continued)

particularly Ca^{2+}, play a very important role in moderating acidity in northeastern China while having a smaller effect in southern China. Moreover, this improvement is only seen for the summer calculations, while the improvement in the calculation of pH values is considerably smaller in winter (Figure 8b). Some of the important processes still need to be better understood, such as the impacts on acidity of very large particles (e.g., $>PM_{10}$,) in urban dust and natural dust storms in northern China.

4. Conclusion

[30] *In situ* pH and soluble ion measurements as well as modeling calculations were undertaken to better understand the nature and causes of atmospheric acidity in China. The results suggest that in northern China, there is a large discrepancy between the major acidity precursors (SO_2 and NO_x) and the measured acidity values (indicated by pH). There are extremely high SO_2 emissions and ambient concentrations in northeastern China, while the acidity is unexpectedly low in this region, resulting in an "inconsistent" situation for acid deposition conditions in this region. This discrepancy was only seen to occur in northern China while in other regions, such as the U.S. and southern China, high SO_2 concentrations are generally well correlated with high acidity values. Using the measured soluble particles (including both acidic and alkaline ions) sampled from 11 city network, we find that there are unusually high levels of alkaline ions in northern China, which play an important role in neutralizing acidity in that region. The results suggest that the high alkaline concentrations, especially Ca^{2+}, can increase summer pH values by about 0.5 in northern China, partially explaining the inconsistency between high sulfate concentrations and low acidity. This result has a very important implication for acid deposition mitigation in northern China. Because the calcium particles in China are mostly the result of dust from natural dust storms and construction activities, the reduction of dust pollution could potentially have the unintended consequence of increasing acid precipitation in northern China. This could possibly occur when, for example, the pace of new construction is significantly reduced in northern China.

[31] This study also suggests that despite the progress made in quantitatively understanding the "inconsistent" situation in northern China, there are still unknown issues

needing further investigation. For example, the reduction of acidity due to the alkaline ions is only significant in summer. During winter, the measured alkaline ions play a much smaller role. We also found that the alkaline ions measured at Xi'An are found largely in the size range from $PM_{2.5}$ to PM_{10}, while even larger particles were not included in the measurements. Because calcium ion concentrations are greater in the larger particles, a significant amount of calcium—a key alkaline ion in northern China—may be underestimated; and importantly, we note that the frequent dust storms that occur in northern China were not sampled (they were explicitly excluded in the sampling protocol used in this study). As a result, dust storms may also be a key factor in understanding the "inconsistency" problem of acid rain in northern China. It should also be noted that the measurements used in this study were obtained in 2003, and updated data would be very useful, both to quantify the current situation and to understand the implications of any changes that may have occurred over the past decade. This all leads to the need for an improved understanding of pollutant-ion-particulate interactions in China and their role in explaining the counter-intuitive conclusion that particulate mitigation strategies in China could have the unintended consequence of exacerbating acid rain conditions.

Appendix A: National Ambient Air Quality Standards for Particulate Matter

U.S. National Ambient Air Quality Standards (http://www.epa.gov/air/criteria.html)

Pollutant [final rule cite]		Primary/ Secondary	Averaging Time	Level	Form
Particle Pollution [71 FR 61144, 17 Oct 2006]	$PM_{2.5}$	primary and secondary	Annual	15 μg/m^3	annual mean, averaged over 3 years
			24 h	35 μg/m^3	98th percentile, averaged over 3 years
	PM_{10}	primary and secondary	24 h	150 μg/m^3	Not to be exceeded more than once per year on average over 3 years

China National Ambient Air Quality Standards[a]

	Averaging Time	Level	Form
PM2.5	Annual	35	Grade II
		15	Grade I
	24 h	75	Grade II
		35	Grade I
PM2.5	Annual	70	Grade II
		40	Grade I
	24 h	150	Grade II
		50	Grade I

[a]Grade I is for natural protection areas and other areas that need special protection; Grade II is for residential, commercial, industrial, and rural areas.

[32] **Acknowledgments.** This work was funded by the National Natural Science Foundation of China (NSFC) under Grant No. 41275168 and 41230641. The National Center for Atmospheric Research is sponsored by the National Science Foundation.

References

Bian, H., X. Tie, J. J. Cao, Z. Ying, and S. Q. Han (2011), Analysis of a severe dust storm event over China: Application of WRF-dust model, *Aero. Air Quality Res.*, *11*, 419–428, doi:10.4209/aaqr.2011.04.0053.

Bond, D. W., S. Steiger, R. Zhang, X. Tie, and R. Orville (2002), The important of NO_x production by lightning in the tropics, *Atmos. Environ.*, *36*, 1509–1519.

Bovensman, H., J. P. Burrows, M. Buchwitz, J. Frerick, S. Noel, V. V. Rozanov, K. V. Chance, and A. P. H. Goede (1999), SCIAMACHY – Mission objectives and measurement modes, *J. Atmos. Sci.*, *56*, 127–150.

Brasseur, G. P., D. A. Hauglustaine, S. Walter, J. F. Muller, P. Rasch, C. Granier, and X. Tie (1998), MOZART: A global three-dimensional Chemical-Transport-Model of the atmosphere, *J. Geophys. Res.*, *103*, 28,265–28,289.

Budhavant, et al. (2012), Atmospheric wet and dry depositions of ions over an urban location in South-West India, *Aerosol Air Qual. Res.*, *12*, 561–570, 2012.

Chan, C. K., and X. H. Yao (2008), Air pollution in mega cities in China, *Atmos. Enviro.*, *42*, 1–42.

Cao, J. J., et al. (2005), Characterization and source apportionment of atmospheric organic and elemental carbon during fall and winter of 2003 in Xi'an China, *Atmos. Chem. Phys.*, *5*, 3127–3137.

Chin, M., R. Rood, S.-J. Lin, J.-F. Müller, and A. M. Thompson (2000), Atmospheric sulfur cycle simulated in the global model GOCART: Model description and global properties, *J. Geophys. Res.*, *105*, 24,671–24,687, doi:10.1029/2000JD900384.

China Meteorological Administration (CMA) (1992), *Manual for Acid Rain Monitoring (in Chinese)*. 2nd ed., pp. 92–105, China Meteorological Administration, Beijing.

China Meteorological Administration (CMA) (2005), *Standard Operation Manual for the Acid Rain Monitoring (in Chinese)*, pp. 10–25, Meteorological Publishing House, Beijing.

Chung, Y. S., H. S. Kim, K. H. Park, J. Dulam, and T. Gao (2005), Observation of dust-storms in China, Mongolia and associated dust falls in Korea in spring 2003, *Water, Air, Soil Pollut.: Focus*, *5*, 15–35.

Emmons, L. K., et al. (2010), Description and evaluation of the model for ozone and related chemical tracers, version 4 (MOZART-4), *Geosci. Model Dev.*, *3*, 43–67.

Gomes, L., and D. A. Gillete (1993), A comparison of characteristics of aerosol from dust storms in central Asia with soil-derived dust from other regions, *Atmos. Environ.*, *27*, 2539–2544.

Horowitz, L. W., S. Walters, D. Mauzerall, L. Emmons, P. Rasch, C. Granier, X. Tie, J. F. Lamarque, M. Schultz, and G. Brasseur (2003), A global simulation of tropospheric ozone and related tracers: Description and evaluation of MOZART, version 2, *J. Geophys. Res.*, *108*, (D24), 4784, doi:10.1029/2002JD002853.

IEA (2010), Key world energy statistics, International Energy Agency.

Kanai, Y., et al. (2005), Characterization of aeolian dust in East China and Japan from 2001 to 2003, *J. of the Meteo. Soc. of Japan*, *83A*, 73–106.

Kawamoto K., T. Hayasaka, T. Nakajima, D. Streets, J. H. Woo (2004), Examining the aerosol indirect effect over China using an SO2 emission inventory, *Atmos. Res.*, *72*, 353–363.

Lu, Z., and D. G. Streets (2011), Sulfur dioxide and primary carbonaceous aerosol emissions in China and India, 1996–2010, *Atmos. Chem. Phys. Discuss.*, *11*, 20,267–20,330. www.atmos-chem-phys-discuss.net/11/20267/2011/, doi:10.5194/acpd-11-20267-2011

Makar, P. A., M. D. Moran, Q. Zheng, S. Cousineau, M. Sassi, A. Duhamel, M. Besner, D. Davignon, L. P. Crevier, and V. S. Bouchet (2009), Modelling the impacts of ammonia emissions reductions on North American air quality, *Atmos. Chem. Phys.*, *9*, 7183–7212.

Safai, P. D., K. B. Budhavant, P. S. P. Rao, K. Ali, and A. Sinha (2010), Source characterization for aerosol constituents and changing roles of calcium and ammonium aerosols in the neutralization of aerosol acidity at a semi-urban site in SW India, *Atmos. Res.*, *98*, 78–88.

Seinfeld, J. H., and S. N. Pandis (2006), *Atmospheric chemistry and physics: From air pollution to climate change*, 2nd ed., pp. 284–343, John Wiley, New York.

Shanghai Municipal Statistics Bureau (SMSB) (2008), *Shanghai Statistical Yearbook*, pp. 78–95, China Statistical Press (in Chinese), Shanghai, China.

Shao, Y., and C. H. Dong (2006), A review in East Asia dust storm climate, modeling and monitoring, *Global Planet. Change*, *52*, 1–22.

Shen, Z. X., J. J. Cao, R. Arimoto, R. J. Zhang, D. M. Jie, S. X. Liu, and C. S. Zhu (2007), Chemical composition and source characterization of spring aerosol over Horqin sand land in northeastern China, *J. Geophys. Res.*, *112*, D14315, doi:10.1029/2006JD007991.

Shen, Z. X., X. Wang, R. J. Zhang, K. F. Ho, J. J. Cao, M. G. Zhang (2011), Chemical composition of water-soluble ions and carbonate estimation in

spring aerosol at a semi-arid site of Tongyu, China, *Aerosol Air Qual. Res.*, *10*, 360–368.

Singer, A. (1988), Illite in aridic soils, desert dusts and desert loses, *Sediment. Geol.*, *59*, 251–259.

Tang J., X. B. Xu, J. J. Ba, S. F. Wang (2010), Trends of the precipitation acidity over China during 1992–2006, *Chinese Sci. Bull.*, *55*, doi:10.1007/s1434-009-3618-1.

Tian H., and J. Hao (2003), Current status and future trend of nitrogen oxides emissions in China, *Prepr. Pap.-Am. Chem. Soc., Div. Fuel Chem.*, *48*(2), pp. 764–765.

Tie, X., G. Brasseur, L. Emmons, L. Horowitz, and D. Kinnison (2001), Effects of aerosols on tropospheric oxidants: A global model study, *J. Geophys. Res.*, *106*, 22,931–22,964.

Tie, X., R. Y. Zhang, G. Brasseur, and W. Lei (2002), Global NO_x production by lighting, *J. Atmos. Chem.*, *43*, 61–74.

Tie, X., S. Madronich, S. Walters, D. P. Edwards, P. Ginoux, N. Mahowald, R. Y. Zhang, C. Lou, and G. Brasseur (2005), Assessment of the global impact of aerosols on tropospheric oxidants, *J. Geophys. Res.*, *110*, D03204, doi:10.1029/2004JD005359.

Tie, X., G. Brasseur, C. Zhao, C. Granier, S. Massie, Y. Qin, P. C. Wang, G. L. Wang, P. C. Yang (2006), Chemical characterization of air pollution in Eastern China and the Eastern United States, *Atmos. Environ.*, *40*, 2607–2625.

Tie, X., D. Wu, and G. Brasseur (2009), Lung cancer mortality and exposure to atmospheric aerosol particles in Guangzhou, China, *Atmos. Environ.*, *43*, 2375–2377.

Tie, X., et al. (2003), Effect of sulfate aerosol on tropospheric NOx and ozone budgets: Evidence during TOPSE, *J. Geophys. Res.*, *108*, 8364.

Wang W. X., and T. Wang (1996), On acid rain formation in China, *Atmos. Environ.*, *30*, 4091–4093.

Wang, Y. Q., X. Y. Zhang, R. Arimoto, J. J. Cao, and Z. X. Shen (2004), The transport pathways and sources of PM10 pollution in Beijing during spring 2001, 2002 and 2003, *Geophys. Res. Lett.*, *31*, L14110, doi:10.1029/2004GL019732.

Xuan J., and I. N. Sokolik (2002), Characterization of sources and emission rates of mineral dust in Northern China, *Atmos. Environ.*, *36*, 4863–4876.

Zhao, C., et al. (2006), Aircraft measurements of cloud droplet spectral dispersion and implications for indirect aerosol radiative forcing, *Geophys. Res. Lett.*, *33*, L11814, doi:10.1029/2006GL025959.